Analytical Methods

Brightfield and fluorescence in-channel staining of thin blood smears generated in a pumpless microfluidic

Journal:	*Analytical Methods*
Manuscript ID	AY-ART-02-2021-000195.R1
Article Type:	Paper
Date Submitted by the Author:	08-Apr-2021
Complete List of Authors:	Dogbevi, Kokou; Texas A&M University System, Biomedical Engineering Gordon, Paul; Texas A&M University College Station, Biomedical Engineering Branan, Kimberly; Texas A&M University System, Biomedical Engineering Ngo, Bryan Khai; Texas A&M University , Biomedical Engineering Kiefer, Kevin ; Texas A&M University College Station, Department of Nutrition and Food Science Talcott, Susanne; Texas A&M Univ., Dept of Veterinary Physiology and Pharmacology Grunlan, Melissa; Texas A+M Univeristy, Biomedical Engineering Cote, Gerard; Texas A&M University, Biomedical Engineering

Brightfield and fluorescence in-channel staining of thin blood smears generated in a pumpless microfluidic.

Received 00th January 20xx,
Accepted 00th January 20xx

DOI: 10.1039/x0xx00000x

www.rsc.org/

Kokou S. Dogbevi,[a*] Paul Gordon,[a*] Kimberly L. Branan,[a] Bryan Khai D. Ngo,[a] Kevin B. Kiefer,[d] Susanne U. Martens-Talcott,[d] Melissa A. Grunlan,[a,b,c,e] Gerard L. Coté [a,e,**]

Effective staining of peripheral blood smears, by increasing contrast of intracellular components and biomarkers, is essential for the accurate characterization, diagnosis, and monitoring of various diseases such as malaria. To assess the potential for automation of stained whole human blood smears at the point-of-care (POC), brightfield and fluorescence staining protocols were adapted for smears generated in channels of pumpless microchannels and compared to a standard glass smear. A 3X concentration Giemsa brightfield staining solutions (10, 33, and 50% dilution), and Acridine Orange fluorescence staining solutions (12 µg/mL) were evaluated with human blood smears containing malaria parasites within a microfluidic channel. Giemsa staining at 33% dilution showed an optimal combination of contrast and preservation of cellular morphology, while 50% dilutions showed significant cellular crenation and 10% dilutions did not show desired contrast in brightfield imaging. Fluorescence staining at 12 µg/mL using Acridine Orange showed clear separability between the fluorescent intensities of the malaria parasites and that of the red blood cells (RBCs) and background. However, compared to glass smears, these exhibited reduced signal intensity as well as inverted contrast of RBCs and background. These results demonstrate that peripheral thin blood smears generated in pumpless microfluidic can be successfully stained in-channel with a simple, one-step, procedures to permit brightfield and fluorescence imaging..

Introduction

The examination of peripheral blood smears via microscopy are essential to the diagnosis of malaria as well as numerous other disease (e.g. anemias, sickle cell diseases, thrombocytopenia, thrombocytosis, leukemia, lymphoma, and iron deficiency).[1-5] This process involves three primary steps: 1) smear generation to produce a monolayer of cells; 2) fixation/staining to accomplish a combination of sample inactivation, permeabilization, adhesion to a substrate, and augmentation with a contrast-enhancing stain; and 3) examination with a microscope, most often fluorescence or brightfield. This work presents the use of a simple staining protocols coupled with a pumpless microfluidic cartridge to permit the fluorescent or brightfield examination of malaria-containing blood smears. Such a device has particular utility at the point-of-care (POC), especially advantageous in medically underserved locations.

Conventionally, for the microscopic diagnosis of malaria, a thin blood smear is manually produced with a drop of blood that is deposited onto a microscope slide and immediately "wiped" across the surface with a second slide to form a monolayer of cells.[6] This process yields variability in the quality of smears created by a single technician and amongst different technicians.[7] After a thin blood smear has been formed and dried, it is fixed using physical or chemical techniques.[8] Fixative chemicals include formaldehyde, glutaraldehyde, acetone, ethanol, methanol, or combinations whereas physical methods are heating, microwaving, and cryo-preservation (freeze-drying).[8-11] Most typically, the smear will be submerged in 100% methanol for 30-60 seconds immediately prior to staining to effectively permeabilize, preserve, and prepare the sample for stain uptake.[12] Some stains, such as Leishman Stain, include fixative agents in their composition and allow for a single-step fixation/staining procedure.[13] Exact fixation protocols vary to account for differences in stain concentration, temperature, osmolarity, and materials used.[14] A proper fixation technique will result in smears that preserve cellular morphology and allow for stain uptake by the sample to produce the desired contrast.[10, 14]

While various types of stains may be used to enhance features of peripheral blood smears, this work focused on the use of Romanowsky-type stain (for brightfield imaging) and Acridine Orange stain (for fluorescence imaging) based on their preference over H&E for inspection of blood cells and their widespread use in malaria detection. Variations in traditional staining protocols arise from variables such as staining compounds, time, concentration, buffers used, pH balance, and age, all of which must be controlled to produce smears with the desired enhanced contrast.[1, 15] Romanowsky and Giemsa-Romanowsky stains are fundamentally a combination of eosin and methylene blue derivatives that create a wide range of blue, purple, and pink hues. Some common examples of these stains include Giemsa, Field's, JSB, Wright's, and Leishman stains, which can be used in numerous distinct ways depending on the sample type and desired effect.[11, 13] The presence of multiple staining compounds is required to create purple hues in what is known as the "Romanowsky effect" within the granules of neutrophils, chromatin, and other cellular matter. Azure B, a methylene blue derivative, is a small molecule that can stain quickly, while eosin, the pigment mainly responsible for the purple color, is three-times bigger and takes longer to diffuse across the cell's membrane, creating a time-hue

[a] *Department of Biomedical Engineering, Texas A&M University, College Station, TX 77843, USA. E-mail: mgrunlan@tamu.edu and gcote@tamu.ed*
[b] *Department of Materials Science & Engineering, Texas A&M University, College Station, TX 77843, USA*
[c] *Department of Chemistry, Texas A&M University, College Station, TX 77843, USA*
[d] *Department of Nutrition and Food Science, Texas A&M University, College Station, TX 77843, USA*
[e] *Center for Remote Health Technologies & Systems, Texas A&M University, College Station, TX 77843, USA*
** Email: gcote@tamu.edu

interdependency that must also be considered.[11] When used in peripheral blood smears, the "Romanowsky effect" is especially visible wherever DNA is present, which causes malarial *Plasmodium* parasites to appear with high contrast due to the lack of DNA in erythrocytes. Similarly, the use of fluorophores in peripheral blood smears has been shown to be viable for parasitic contrast enhancement within red blood cells (RBCs), with some studies claiming greater sensitivity with the use of fluorescent stains when compared to brightfield-chromophores.[16-20] Acridine Orange is a cell-permeant stain that bonds to DNA and RNA via intercalation with fluorescent emission peaks of 526 nm and 650 nm, respectively. It has been used in malaria research and diagnosis due to its combination of function, cost, and stability.

Use of either a brightfield or fluorescent stain requires a balance between maximizing stain-target binding and saturating the thin blood smear such that binding specificity and contrast is lost.[1] In Romanowsky-stained blood smears, under-staining results in highly transparent samples with poor contrast, and over-staining results in nearly homogenous light absorption across entire cells such that little to no chromatic variance between targets and the cellular background can be seen. Acridine Orange-stained smears, which are imaged through filters to block all non-signal light, do not emit sufficient photons to generate a discernable signal when under-stained, and overstaining results in fluorescence being seen in sample background, cellular membranes, and condensed debris, creating washed-out images. Poor smear fixation and staining should be avoided whenever possible to mitigate diagnostic errors that can lead to incorrect diagnoses and treatment, ultimately increased morbidity, mortality as well as socio-economic burden.[2, 15, 21-24] Since diagnostic errors oftentimes are attributed to stain quality, automated staining devices have been developed (e.g. automated slidemakers and paper fluidic devices) but most are typically unsuitable for use at the POC, away from centralized laboratories, because they tend to be cumbersome and expensive.[25, 26] One automated slidemaker device by Horning et.al had a simplified design and was reasonably well suited for fluorescence imaging; however, it lacked optical transparency necessary for bright field imaging. Thus, there is a need for an automated or semi-automated staining platform technology and simple protocols that can incorporate a diverse set of stains, particularly for use at the POC.[1, 15]

A pumpless microfluidic for automated blood smear generation that can be coupled to an automated fixation and staining process would represent a major advancement in the diagnosis and detection of malaria and other diseases at the POC. Microfluidic systems have been proposed as they offer low-cost, adaptable, rapid, and easy-to-use detection platforms for various biological analytes.[27, 28] However, the use of a single microfluidic chip to simultaneously accomplish smear generation, fixation, and staining require complex auxiliary technologies to operate and fail to meet the World Health Organization's ASSURED criteria or FDA simple test guidance.[28, 29] For instance, Li et al. showed that blood smears can be stained in a microchannel but required pumps and valves to do so and straining produced many artifacts.[30] Horning et al. designed a blood smear staining device on a paper microfluidic cartridge; however, the lengthy drying times required does not meet the WHO's ASSURED criteria, which requires that the diagnosis procedure be done in under 30 min.[29, 31] Additionally, the use of paper-fluidics causes difficulty in achieving the necessary microscopy resolution for accurate disease diagnosis.

We previously demonstrated the pumpless capillary flow of blood in microfluidic chips prepared with an amphiphilic silicone.[32] To fabricate these microchannels, Sylgard 184 was readily bulk modified a surface modifying additive (SMA), a poly(ethylene oxide) (PEO) silane amphiphile comprised of a crosslinkable silane (Si-H) group, an oligodimethylsiloxane (ODMS) tether, and a PEO segment: $HSi\text{-}PDMS_{30}\text{-}PEO_8\text{-}OCH_3$. The rapid and substantial migration of PEO segments to the channel surface/blood interface led to "on demand" surface hydrophilicity and increased SMA concentration produced a greater rate of capillary flow. Furthermore, versus unmodified Sylgard 184, the amphiphilic silicones exhibited only a slight increase in light attenuation and nearly no autofluorescence. More recently, by including pillar sections at the inlet, outlet and two interior regions, a uniform thin blood smear could be consistently achieved in under 10 minutes.[33] Staining a blood smear within a microfluidic channel poses a unique situation. Manually-generated blood smears manually produced on microscope slides are first dried and fixed prior to staining. As a closed system, it is difficult and time-consuming for smears in microchannels to dry between reagent steps and so staining must be done in liquid-phase suspension.

Herein, wet, in-channel staining protocols were developed for Romanowsky and Acridine Orange brightfield and fluorescent staining, respectively, of thin blood smears generated in a pumpless microfluidic channel. Microfluidic chips were prepared based on our prior reports using an amphiphilic silicone (Sylgard 184 with 7 wt% $HSi\text{-}PDMS_{30}\text{-}PEO_8\text{-}OCH_3$ SMA) and pillar-containing channel design. Human blood was cultured with *P. falciparum* malarial parasites. The parasitized blood was combined with a staining solution of varying concentrations and then deposited into a microfluidic channel. The concurrent generation of the thin blood smear and fixing/staining as well as the lack of drying required permitted specimens to be ready for imaging in under 20 min. To assess staining quality, image analysis was performed in terms of quantitative feature of separability of parasites from both intracellular and extracellular backgrounds. Results were compared to those obtained with using traditional methods to manually generate a thin blood smear on a glass slide and to fix/stain the smear.

Materials and methods

Preparation of staining solutions. A Giemsa powder and Acridine Orange powder (Millipore-Sigma) were used for all brightfield and fluorescence stain solution preparations, respectively. Giemsa 3X concentration stock solution was made using the protocol described by Bain et al, modified to use 300 mg of Giemsa powder mixed with 10 mL of absolute methanol (Sigma).[34] The mixture was put on a hot plate at 50 °C for 15 min. Next, the stock was put on a mixer for at least 12 hr thoroughly dissolve the Giemsa powder. The stock was then sequentially filtered using 4 µm and 2 µm paper filters. The filtered stock was left sitting for at least 24 hr before use. Acridine orange (AO) stock solution was made as a 96 µg/mL suspension of AO in 1X PBS pH 7.2 (147 mM NaCl, 2.7mM KCl, 10mM PO_4^{3-}; VWR Chemicals).

***Preparation of microfluidic chips with amphiphilic silicone*.** Microfluidic thin-smear generating cartridges were prepared according to protocols described in or previous work.[32, 33] Details are summarized in the Supplemental Information (Part A). Briefly, the microfluidic chips contained four equivalent channels (~300 µm wide, ~4.7 µm height, ~14 µm long), D-shaped channels with the curved portion (facing the bottom) made of the amphiphilic silicone and the flat portion (facing the top) was the glass slide to which it was bonded (Figure S1). Within each channel were a series of pillars (50 µm diameter, 25 µm gap between pillars, ~4-5 horizontal rows) at four different locations: at the inlet, at the outlet, as well as at two locations approximately 4 mm and 8 mm from the inlet. The series of pillars located at the inlet and outlet spanned a length of ~1.2 mm and was comprised of ~17 vertical columns of pillars; however, this was reduced to ~12 columns upon creating a 5 mm well with a biopsy punch at the inlet and the outlet. The interior series of pillars occupied a length of ~184 µm and also consisted of ~3 vertical columns of pillars.

***Culture of P.* falciparum parasites**. *P. falciparum* parasites were cultured *in vitro* and reconstituted to mimic physiological properties of unaltered human blood according to details noted in Supplemental Information (Part B). All studies were conducted in compliance with relevant laws and institutional guidelines. The human blood used for parasite culture and sample reconstitution (Figure S2) was donated under exemption approval from the Texas A&M Institutional Review Board. No human subjects were involved in the work.

Staining protocols and imaging. To serve as controls, manually prepared blood smears were prepared on glass microscope slides and subsequently fixed and stained with both brightfield (Giemsa) and fluorescence (Acridine Orange) stains according to published procedures.[6, 17-19, 35] To summarize, a single drop of blood was placed on a clean microscope slide, and then wiped across the surface using a second slide to create a thin cell monolayer. Once air-dried, the smears were fixed by dipping in methanol for 10 sec and allowing to air dry. Subsequent staining was performed by submersion of the microscope slide into the designated staining solution, followed by briefly rinsing with DI water.

For in-channel fixing and staining of thin blood smear created in microfluidic channels, the following protocol was utilized. For brightfield staining, a 3X Giemsa stain stock concentration was diluted with DI water to create 10%, 33%, and 50% by volume stain solutions. Fluorescence stain solutions were created by diluting AO to concentrations of 96 µg/mL, 24 µg/mL, 12 µg/mL, and 6 µg/mL in 1X PBS. Stain-blood solutions were prepared by mixing stain solutions with reconstituted parasitized blood in 1:2 (stain solution:blood) by volume in 2 mL centrifuge tubes. These were mixed by hand for 30 sec then set aside under a light-shielding covering for 10 min to incubate at RT. After 10 min, 0.5 µL was transferred to the inlet of the microfluidic channel via pipette. After cells stopped flowing in the channels 4.31 ± 0:39 min), imaging commenced. A Nikon Eclipse Ti-2 microscope with 60X oil-immersion objective was used to take images of the cells from the outlet to the inlet at 0.5 mm increments, and the images were catalogued for later analysis.

Image analysis. Image analysis was performed to compare staining quality, which was defined as the quantitative feature of separability of parasites from both intracellular and extracellular backgrounds. Brightfield images contained standard red, green, and blue (RGB) data while fluorescence images were monochromatic. Images from each mode of imaging were processed similarly, with parasitic, RBC, and background features segmented using masks that were commonly applied to all images taken for individual single staining procedures. For brightfield images, MATLAB was used to segment parasites, RBCs, and background using hue, saturation, and value (HSV). HSV are alternative representations of the RGB color model designed to more closely align with the way human vision perceives color-making attributes.[36-38] In these models, colors of each hue are arranged in a radial slice, around a central axis of neutral colors which ranges from black at the bottom to white at the top.[39] Within this study, HSV is represented in cylindrical coordinates where hue is the angular component ranging from 0 - 360°, saturation is the radial component ranging from 0-1, and value is indicated by the height from 0-1. Feature differentiability was determined from the HSV values of each feature's pixel population. When plotted in cylindrical HSV color space, the distance between population clusters were compared, with larger distances indicating that features were more differentiable. The quantitative variance of stained features was used to assess overall repeatability both within and between images gathered from each individual smear. Throughout all portions of image analysis, cellular morphology was qualitatively assessed to ensure that no crenation, lysis, or significant morphological deformations occurred at any point during the staining process or tests. In fluorescence images, parasitic, RBC, and background features were segmented using Nikon BR Elements software based on the presence of intensity thresholded local maxima in

the imaging field, and the intensities of these features were analyzed for separability and repeatability.

Results and discussions

In-Channel Brightfield Staining

The selected lower (10%) and upper (50%) percent Giemsa concentrations for the staining solutions were selected based on the conventional procedures that typically use a 10% concentration and deformations in cellular morphology that appeared above 50% concentration. For Giemsa stained samples (Figure 1; Table 1), HSV values for smear background, RBCs, and malaria parasites were found by averaging 10 brightfield images for each of the stain solution concentration. For all staining concentrations, malaria parasites representing comparable blue colors. However, the background and RBCs result in slightly different shades of gray with the 10% stain solution resulting in the lightest shade of gray.

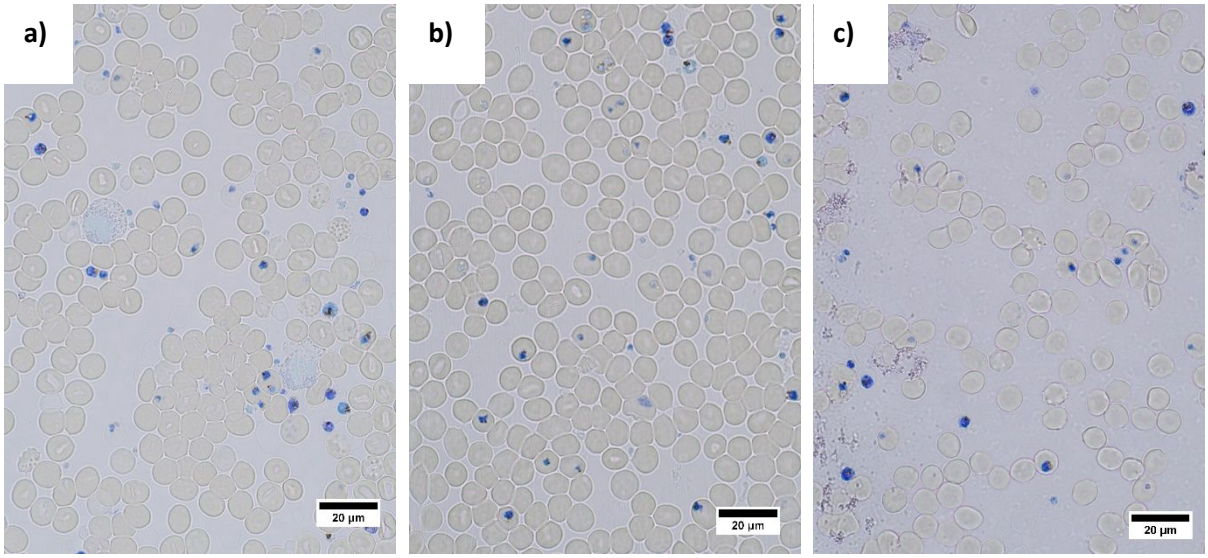

Figure 1: Images of in-channel, Giemsa stained blood smears using (a) 10% Giemsa stain ing solution; (b) 33% Giemsa staining solution; (c) 50% Giemsa staining solution.

Table 1: Average HSV intensities with standard deviations (STD) for the background, RBCs, and malaria parasites from 10 images obtained with 10%, 33%, and 50% Giemsa staining solutions.

Average HSV for 10 images each	**Background** H ± STD S ± STD V ± STD	**RBCs** H ± STD S ± STD V ± STD	**Malaria** H ± STD S ± STD V ± STD
10% Giemsa staining solution	237.942 ± 1.647 0.048 ± 0.004 0.776 ± 0.003	236.988 ± 0.624 0.051± 0.005 0.776 ± 0.004	210.24 ± 1.742 0.396 ± 0.03 0.663 ± 0.009
33% Giemsa staining solution	243.972 ± 1.528 0.058 ± 0.006 0.798 ± 0.008	194.076 ± 15.02 0.03 ± 0.001 0.706 ± 0.005	216.114 ± 0.775 0.478 ± 0.02 0.666 ± 0.016
50% Giemsa staining solution	236.196 ± 2.407 0.071 ± 0.008 0.781 ± 0.004	147.664 ± 9.306 0.036 ± 0.004 0.715 ± 0.007	220.356 ± 6.333 0.533 ± 0.023 0.656 ± 0.045

In HSV color space, the feature separability increases with the stain concentration as shown by the increased average magnitude of distances between the malaria parasites and the background for the 10% (circles), 33% (triangles), and 50% (squares) Giesma stain solutions (Figure 2). Although the distance between the background and malaria parasite is

greatest for the 50% staining solution, more cells show crenation at this dilution (i.e. the RBCs underwent shrinkage and acquired a notched or scalloped surface) than observed with 33% and 10% staining solution (Figure 1). This is likely due to the higher methanol concentrations used in the 50% stain. In addition, with a 10% staining solution, there was considerable overlap in the background and RBC values (yellow and red circles), whereas the 33% and 50% dilutions showed good separation (Figure 2b). Overall, the results indicate that the 33% Giemsa staining solution gives an optimal of enhanced contrast between all three features (background, RBCs, and malaria parasites) and preserved cellular morphology that is preferable for brightfield staining.

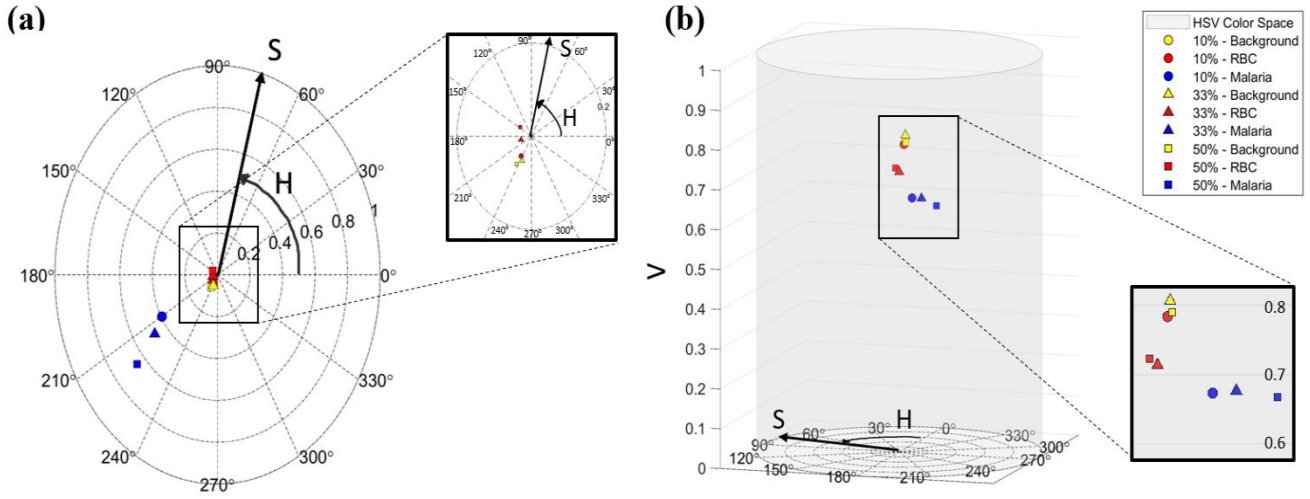

Figure 2: Average HSV colors for malaria parasites (blue), background (yellow), and RBCs (red) from 10 brightfield images for (a) a 2D hue and saturation space and (b) a 3D hue, saturation, and value space per 10% (circles), 33% (triangles), and 50% (squares) Giemsa staining solutions.

Comparison of In-Channel Brightfield Staining Across Different Channels and Within a Channel

Multiple independent trials of the 33% Giemsa staining protocol were performed to assess consistency of staining, both among three different channels prepared on the same chip and within a given channel. Color and color differentiation were found to be consistent across all three channels (Figure 3). The average HSV results from 10 images within each channel (in terms of background, RBCs, and malaria parasites) are depicted in Figure 4. In addition, Figure 5 shows the HSV variation across three

channels from 10 images within each channel. Table 2 shows the quantitative HSV values within and across channels and, although the hue angle across the three channels varies considerably for the RBCs, the saturation and value levels are consistent yielding a grouping that is tight in the 3D plot of Figure 5. Overall, as depicted in Figure 4 and 5, the distances within the HSV color space for the background, the RBCs and the malaria parasites for the 10 images within each channel and across channels have no significant difference, which shows the consistency of the 33% staining solution protocol. Further, there is no overlap within and across channels between the background, RBCs, and malaria parasites showing excellent separation and hence color contrast (Figures 4 & 5) both within and across channels for the 33% staining solution.

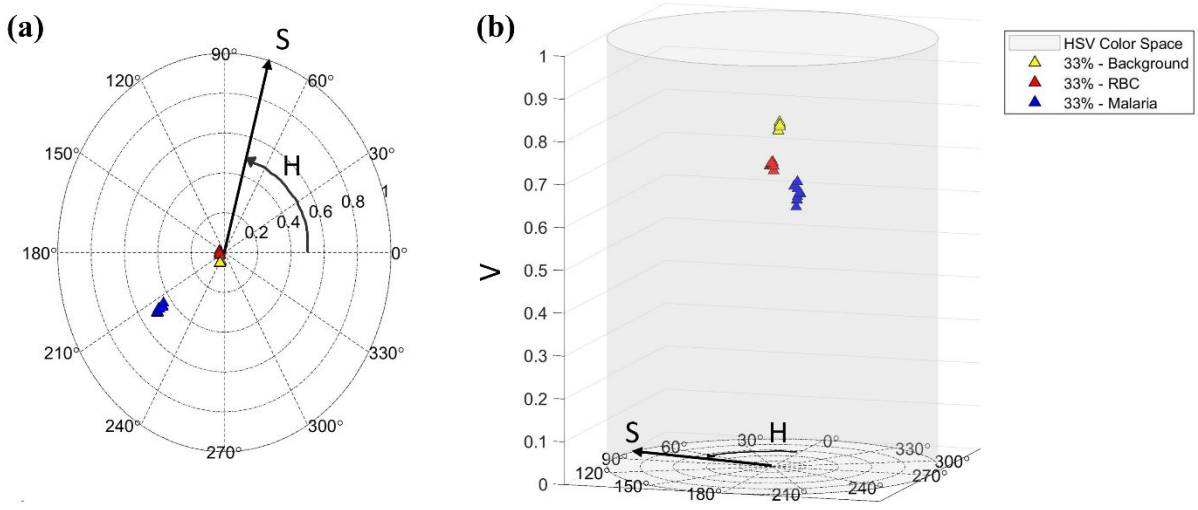

Figure 4: Within a channel, average HSV colors for the malaria parasites (blue), the background (yellow), and the RBCs (red) from 10 images for a) 2D hue and saturation space and b) 3D hue, saturation, and value space for the 33% Giemsa stain solution.

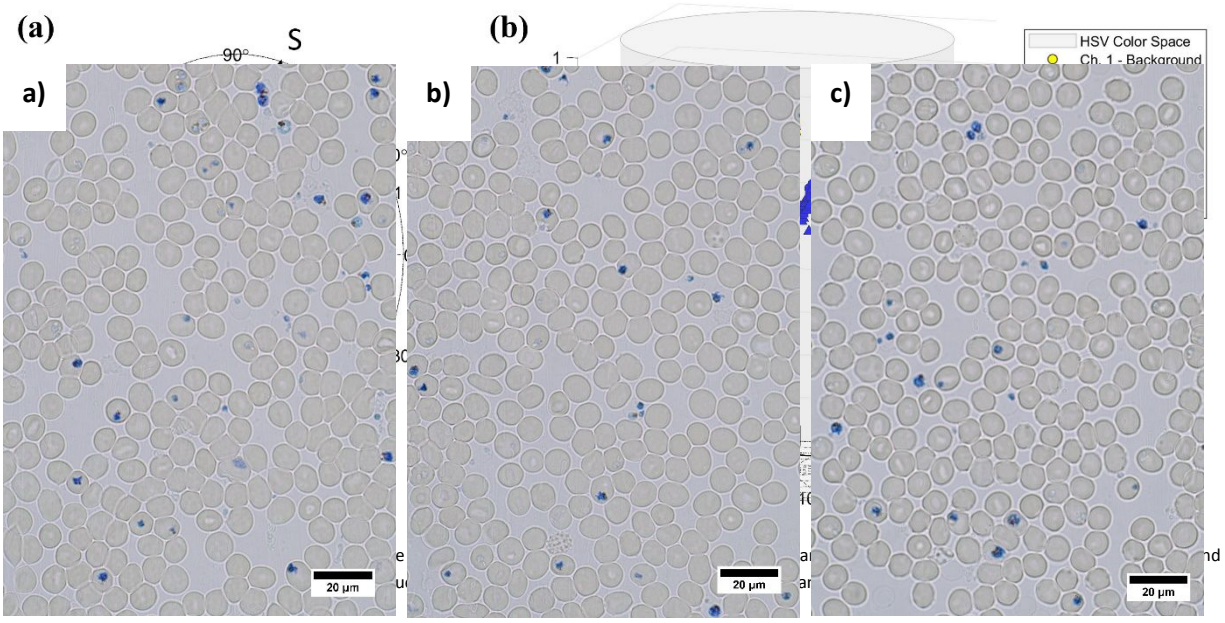

Figure 3: Representative images of malaria parasites acquired from 33% Giemsa stain solutions in three different channels (Ch) of a chip: a) Ch-1; b) Ch-2; and c) Ch-3.

Table 2: Average HSV intensities with standard deviations (STD) for the background, RBCs, and malaria parasites for 10 images within three channels (Ch) created by the 33% Giemsa stain solution.

Average HSV for 10 images each	**Background** H ± STD S ± STD V ± STD	**RBCs** H ± STD S ± STD V ± STD	**Malaria** H ± STD S ± STD V ± STD
Channel 1	243.972 ± 1.528 0.058 ± 0.006 0.798 ± 0.008	194.076 ± 15.02 0.030 ± 0.001 0.706 ± 0.005	216.114 ± 0.775 0.478 ± 0.02 0.666 ± 0.016
Channel 2	243.792 ± 1.159 0.053 ± 0.008 0.784 ± 0.012	210.24 ± 8.417 0.032 ± 0.002 0.704 ± 0.006	212.796 ± 1.915 0.447 ± 0.035 0.637 ± 0.029
Channel 3	239.184 ± 2.912 0.069 ± 0.009 0.79±0.006	149.08 ± 8.608 0.033 ± 0.003 0.698 ± 0.007	219.204 ± 5.336 0.452 ± 0.028 0.676 ± 0.041
Average Across Channels	242.376 ± 1.866 0.06 ± 0.008 0.791 ± 0.009	184.465 ± 10.682 0.032 ± 0.002 0.703 ± 0.006	216.038 ± 2.675 0.459 ± 0.277 0.66 ± 0.029

Comparison of In-Channel Brightfield Staining to Staining of Manually Prepared Glass Smears

The aforementioned results obtained with in-channel staining with a 33% Giemsa solution was compared to a conventional control prepared on a glass slide. Background, RBC, and malaria parasite HSV values for the glass smears and in-channel smears are reported in Table 3. The clustering within the background, RBC, and malaria parasite space is quite good as well as the separability across the HSV space between these three characteristics (Table 3, Figure 6). Notably, although both approaches show good separability with high signal to noise, the glass smear had a slightly higher standard deviation in the grouping of the malaria parasites particularly in the hue value. The hue variance of stained parasites is the result of differing binding affinities between competing chromophores in the Giemsa stain, resulting in a wide range of colors useful for the differentiation of various morphological characteristics such as early and late stage parasitic forms. It is difficult to isolate the direct source of the differing hue variance between glass smears and in-channel stained samples, which could result from either altered chromophore competitive binding dynamics or from the inclusion of highly hue-variant white blood cells or late stage parasites in images. Overall, as depicted in the representative images for the stained glass smear and the stained in-channel smear (Figure 7), the biggest difference is in the color of the glass smears' RBCs (purple) and the in-channels' RBCs (grey). This phenomenon shows up in the HSV color space, with large differences in the Hue and Saturation for the RBCs (Table 3). This makes the differentiation between the RBCs and malaria parasites more striking in the in-channel smear. It consequently also makes the background more distinguishable from the RBCs in the glass smear. Overall, the malaria parasites,

Table 3: Average HSV intensities with standard deviations (STD) for the background, RBCs, and malaria parasites from 10 images for the glass smear and in-channel smear.

Average HSV for 10 images each	**Background** **H±STD** **S±STD** **V±STD**	**RBCs** **H±STD** **S±STD** **V±STD**	**Malaria** **H±STD** **S±STD** **V±STD**
Glass smear treated with Giemsa stain	243.174 ± 1.114 0.078 ± 0.0003 0.778 ± 0.002	303.492 ± 2.498 0.079 ± 0.0020 0.62 3± 0.0059	238.943 ± 2.924 0.384 ± 0.0182 0.685 ± 0.0127
In-channel smear with 33% Giemsa stain solution	243.972 ± 1.528 0.058 ± 0.006 0.798 ± 0.008	194.076 ± 15.02 0.03 ± 0.001 0.706 ± 0.005	216.114 ± 0.775 0.478 ± 0.02 0.666 ± 0.016

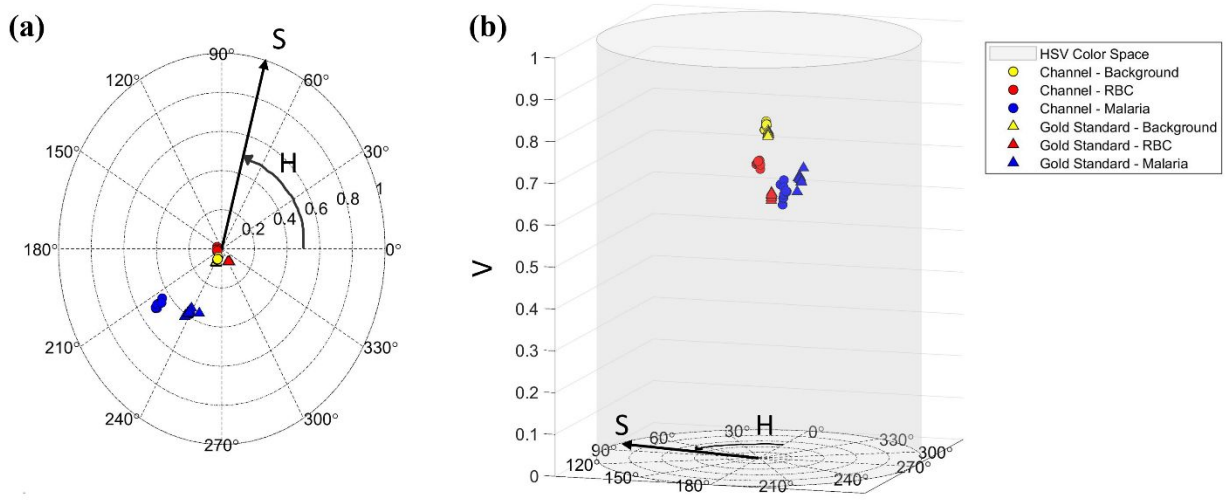

Figure 6: Average HSV colors for the malaria parasites (blue), the background (yellow), and the RBCs (red) for 10 images within a) 2D hue and saturation space and b) 3D hue, saturation, and value space per the 33% (circles) and gold standard (triangles) staining protocols.

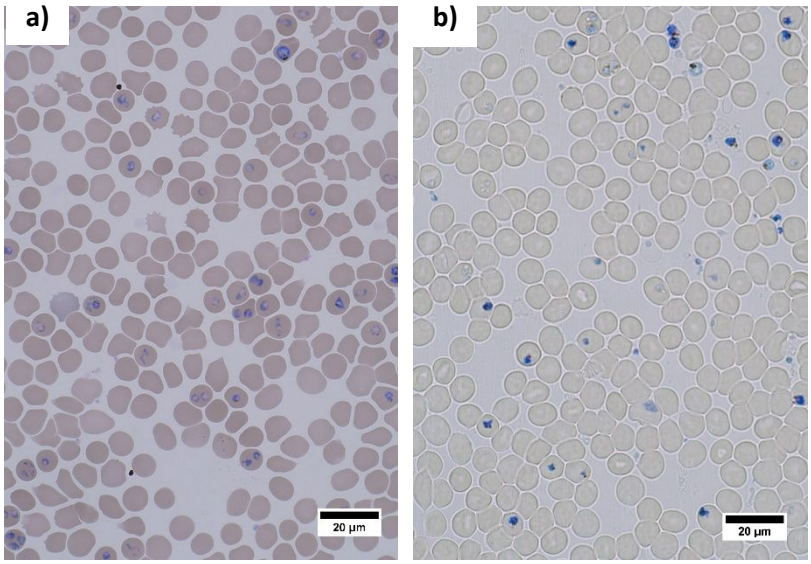

Figure 7: Images of blood smears and malaria parasites acquired from a) glass smear with Giemsa staining; and b) in-channel smear with 33% Giemsa stain solution.

RBCs, and background are as distinguishable from each other in the microfluidic channels versus the conventional glass smear.

.

In-Channel Fluorescent Staining

Fluorescently stained samples were imaged in a similar manner to the brightfield images, with eight images collected at 0.5 mm intervals across the channel, beginning 10 min after cells were stained. Acridine Orange (AO) stain solution at 12 µg/mL was used to stain both in-channel and glass smear controls. This concentration was chosen due to its ability to reliably stain the glass smears with high contrast and little saturation. Signal intensities for all AO concentrations can be found in Supplemental Information (Part C) (Figures S3, S4). In each, the uptake of AO by parasites allowed them to be clearly seen above the RBCs and background signals (Figure 8). Using a 16-bit monochromatic camera, parasitic features in the microchannel displayed smaller intensities near 4000, while glass smears displayed intensities near 14000. Background, RBC, and malaria parasites from both the glass and channel-

based smears display similar coefficients of variation as determined across eight images down the channel and showed separability when normalized (Figure 9). However, for smears generated in the microchannel, the RBC's appear darker than the channel background, while in the glass smear images, they appear brighter than the background (Figure 8). This is likely due to the ability of excess fluorophores to be washed away from glass-mounted smears but not from microchannel smears. Despite these differences, in each image, there was a clear separability between the fluorescent intensities of the malaria parasites and those of the RBC's and background (Figure 9).

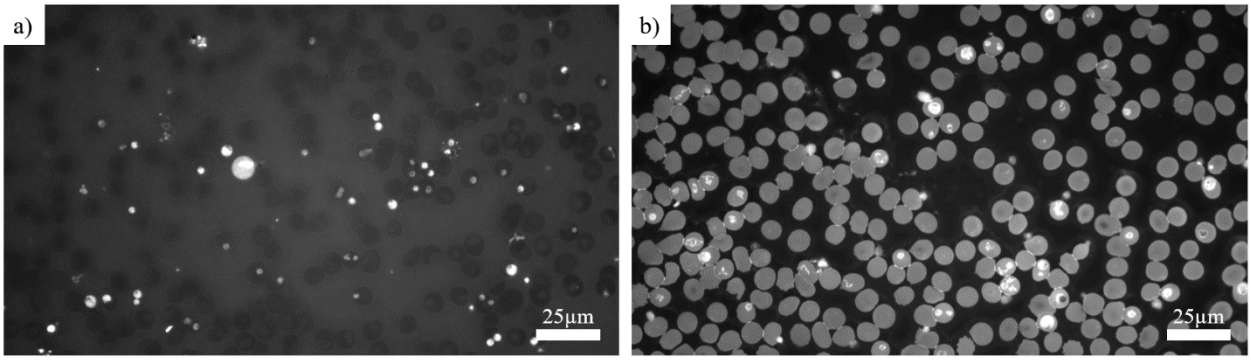

Figure 8: Monochromatic images of samples stained using 12µg/mL Acridine Orange a) in-channel; and b) glass smear. Parasites appear brightly in both images, but the contrast of RBCs and the background are inverted. The images are shown with linear contrast enhancement for visibility.

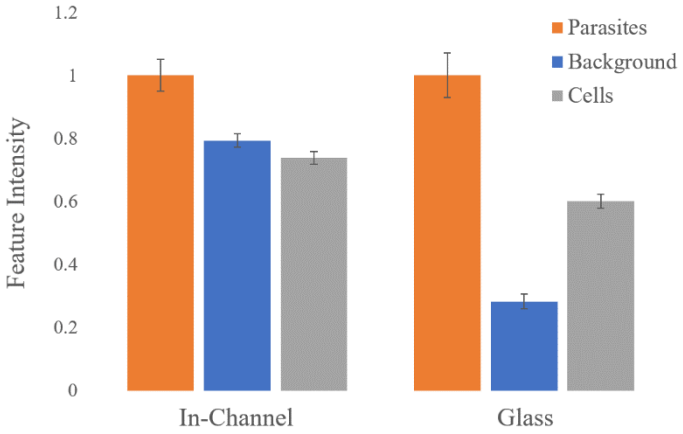

Figure 9: Comparison of relative fluorescent feature intensities from in-channel and glass smear samples stained with 12 µg/mL of Acridine Orange. Error bars represent variance of entire feature population across all images.

Comparison of In-Channel Fluorescent Staining Across Within a Channel and Across Different Channels

Three independent repetitions of the staining and smear creation process were performed for the 12 µg/mL stain concentration to assess the repeatability of the process. Feature intensity variance was compared within each field-of-view (FOV) and between independently stained channels. The average relative feature intensities of parasites, background, and RBC's remain consistent throughout the channel (Figure 10a). To better assess staining quality as defined by feature separability, intensities in each FOV were normalized to the intensity of the background to eliminate linear baseline drift that occurred as a gradient along the channel. Due to the differential uptake of stain by parasites of various stages of development and the heterogeneity of fluorescence staining within each individual parasite, a large standard deviation can be observed in the average intensities of populations of parasites from each FOV, however the precision afforded by sampling multiple FOV allows for the clear separation between

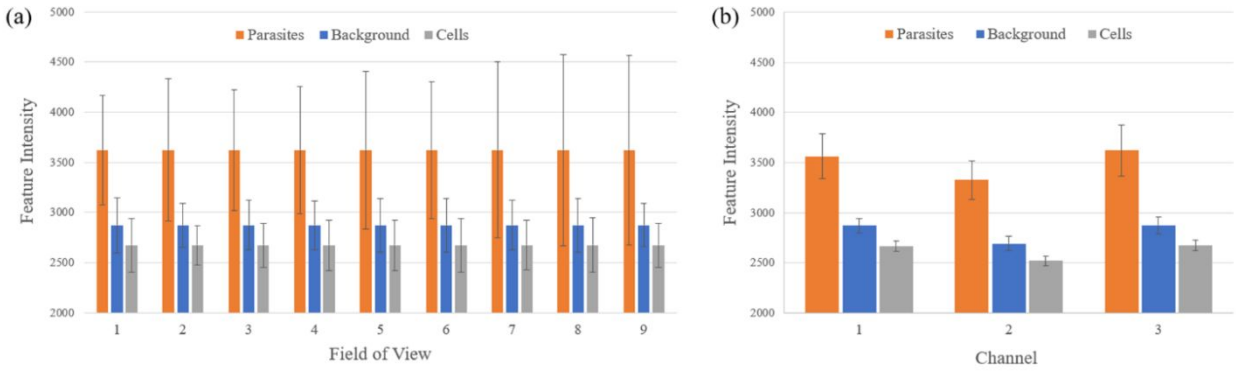

Figure 10: Fluorescence staining: a) within a single channel, and b) between three separate, independent channels.

the intensities of parasites, RBC's and background in all three channels (Figure 10b).

Conclusion

In this work, peripheral thin blood smears containing *P. falciparum* malaria parasites were generated in pumpless microfluidic channels and subsequently subjected to in-channel staining to permit brightfield and fluorescent imaging. The in-channel, wet staining results were compared to those of glass smears which are dried prior to staining. For in-channel staining, a 3X concentration Giemsa brightfield staining solutions (10, 33, and 50% dilution), and Acridine Orange fluorescence staining solutions (12 µg/mL) were used. Staining quality was assessed quantitatively using chromatic and intensity-based feature differentiation for brightfield and fluorescence imaging modalities, respectively. A 33% Giemsa staining solution afforded the best contrast and preserved cellular morphology, with consistent results afforded within a channel and among different channels. Overall, the malaria parasites, RBCs, and background (i.e. plasma) in the microfluidic channels are similarly distinguishable from each as for conventional Giemsa-stained glass smears. Following in-channel fluorescence staining, malaria parasites could be consistently distinguished from the RBCs and background but had reduced signal intensity as well as inverted contrast of RBCs and background versus Acridine Orange-stained glass smears. The ability to effectively stain thin blood smears generated in a pumpless microfluidic represents a significant step towards diagnosis of malaria and other diseases at the POC.

Acknowledgements

G.L.C. gratefully acknowledge support from the National Science Foundation (#1402846). K.S.D. gratefullyacknowledges support from the National Science Foundation (#HRD-1502335). All authors acknowledge support from the Texas A&M Engineering Experiment Station (TEES).

Associated content

Supporting Information. Supporting Information is available free of charge at [website]. Fabrication of microfluidic chips including PEO-silane synthesis and mask design and fabrication; reconstitution of malaria cultures; effect of varying Acridine Orange stain concentration

Author Information

*These authors contributed equally.

Corresponding Author
**Email: gcote@tamu.edu
ORCID: 0000-0002-3164-9625

Notes

The authors declare no competing financial interests.

References

1. A. S. Adewoyin and B. Nwogoh, *Ann Ib Postgrad Med*, 2014, **12**, 71-79.
2. B. J. Bain, *N Engl J Med*, 2005, **353**, 498-507.
3. G. Gulati, J. Song, A. D. Florea and J. Gong, *Annals of laboratory medicine*, 2013, **33**, 1-7.
4. J. A. Kull, P. D. Krawczel and G. M. Pighetti, *Vet Immunol Immunop*, 2018, **197**, 21-23.
5. S. R. Comar, M. Malvezzi and R. Pasquini, *Rev Bras Hematol Hemoter*, 2017, **39**, 306-317.
6. W. H. Organization, *Basic malaria microscopy: Part I. Learner's guide*, World Health Organization, 2010.
7. J. D. Maguire, E. R. Lederman, M. J. Barcus, W. A. P. O'Meara, R. G. Jordon, S. Duong, S. Muth, P. Sismadi, M.

J. Bangs, W. R. Prescott, J. K. Baird and C. Wongsrichanalai, *Malaria journal*, 2006, **5**, 92-92.
8. I. Eltoum, J. Fredenburgh, R. B. Myers and W. E. Grizzle, *J Histotechnol*, 2001, **24**, 173-190.
9. L. Benattar and G. Flandrin, *J. Leuk. Lymphoma*, 1999, **33**, 587-591.
10. G. Rolls, *Fixation and*, 2012.
11. R. W. Horobin, *Biotechnic & histochemistry : official publication of the Biological Stain Commission*, 2011, **86**, 36-51.
12. B. Houwen, *Clin Lab Med*, 2002, **22**, 1-14.
13. S. Sathpathi, A. K. Mohanty, P. Satpathi, S. K. Mishra, P. K. Behera, G. Patel and A. M. Dondorp, *Malaria journal*, 2014, **13**, 512-512.
14. H. Singh, K. A. Bishen, D. Garg, H. Sukhija, D. Sharma and U. Tomar, *Dent. J. Adv. Stud.*, 2019, **07**, 051-055.
15. M. P. Horning, C. B. Delahunt, S. R. Singh, S. H. Garing and K. P. Nichols, *Lab Chip*, 2014, **14**, 2040-2040.
16. F. Kawamoto, *The Lancet*, 1991, **337**, 200-202.
17. C. Wongsrichanalai, J. Pornsilapatip, V. Namsiripongpun, H. K. Webster, A. Luccini, P. Pansamdang, H. Wilde and M. Prasittisuk, *Am. J. Trop. Med. Hyg.*, 1991, **44**, 17-20.
18. B. Lowe, N. Jeffa, L. New, C. Pedersen, K. Engbaek and K. Marsh, *Trans R Soc Trop Med Hyg*, 1996, **90**, 34-36.
19. R. Guy, P. Liu, P. Pennefather and I. Crandall, *Malaria Journal*, 2007, **6**, 89-89.
20. S. M. Parsel, S. A. Gustafson, E. Friedlander, A. A. Shnyra, A. J. Adegbulu, Y. Liu, N. M. Parrish, S. A. Jamal, E. Lofthus, L. Ayuk, C. Awasom, C. J. Henry and C. P. McArthur, *Infect Dis Poverty*, 2017, **6**, 32.
21. M. Amexo, R. Tolhurst, G. Barnish and I. Bates, *The Lancet*, 2004, **364**, 1896-1898.
22. C. Wongsrichanalai, M. J. Barcus, S. Muth, A. Sutamihardja and W. H. Wernsdorfer, *Am J Trop Med Hyg*, 2007, **77**, 119-127.
23. J. E. Hyde, *FEBS J*, 2007, **274**, 4688-4698.
24. H. A. Antony and S. C. Parija, *Trop. Parasitol*, 2016, **6**, 30-41.
25. E. Simson, M. G. Gascon-Lema and D. L. Brown, *Int J Lab Hematol*, 2010, **32**, e64-76.
26. G. K. Rumindo, M. Panjaitan and A. Djajadi, 2011.
27. G. M. Whitesides, *Nature*, 2006, **442**, 368-373.
28. A. Manz, D. J. Harrison, E. M. J. Verpoorte, J. C. Fettinger, A. Paulus, H. Lüdi and H. M. Widmer, *J. Chromatogr. A*, 1992, **593**, 253-258.
29. S. M. Hattersley, J. Greenman and S. J. Haswell, in *Microfluidic Diagnostics: Methods and Protocols*, eds. G. Jenkins and C. D. Mansfield, Humana Press, Totowa, NJ, 2013, DOI: 10.1007/978-1-62703-134-9_19, pp. 285-303.
30. H. Li, H. Jayamohan, C. Lambert, S. Mohanty and B. Gale, *Automated Whole Blood Processing With a Portable Microfluidic Device for Point-of-Care Diagnosis 2013.*
31. R. W. Peeling, K. K. Holmes, D. Mabey and A. Ronald, *Sex Transm Infect*, 2006, **82 Suppl 5**, v1-v6.
32. K. S. Dogbevi, B. K. D. Ngo, C. W. Blake, M. A. Grunlan and G. L. Coté, *ACS Appl Polym Mater*, 2020, DOI: 10.1021/acsapm.0c00249.
33. K. S. Dogbevi, B. K. D. Ngo, K. L. Branan, A. M. Gibbens, M. A. Grunlan, G. L. Coté "A thin whole blood smear prepared via a pumpless microfluidic," *in review.*
34. B. J. Bain and S. Mitchell Lewis, in *Dacie and Lewis Practical Haematology (Tenth Edition)*, eds. S. M. Lewis, B. J. Bain and I. Bates, Churchill Livingstone, Philadelphia, 2006, DOI: https://doi.org/10.1016/B0-44-306660-4/50008-8, pp. 59-77.
35. J. Keiser, J. Utzinger, Z. Premji, Y. Yamagata and B. Singer, *Ann Trop Med Parasitol*, 2002, **96**, 643-654.
36. H. Dasari and C. Bhagvati, 2007.
37. D. J. Bora, A. K. Gupta and F. A. Khan, *arXiv preprint arXiv:1506.01472*, 2015.
38. C. Junhua and L. Jing, 2012.
39. B. Peswani, *International Journal for Scientific Research and Development*, 2014, **1**, 2631-2634.

1